ORIGINAL RESEARCH

Wnt Signaling in Chronic Rhinosinusitis with Nasal Polyps

Robert Böscke[1,2*], Eszter K. Vladar[3*], Michael Könnecke[1], Birgit Hüsing[1], Robert Linke[1], Ralph Pries[1], Norbert Reiling[4], Jeffrey D. Axelrod[3], Jayakar V. Nayak[2], and Barbara Wollenberg[1]

[1]Department of Otolaryngology, Head and Neck Surgery, University of Lübeck, Lübeck, Germany; [2]Department of Otolaryngology, Head and Neck Surgery, and [3]Department of Pathology, Stanford University School of Medicine, Stanford, California; and [4]Division of Microbial Interface Biology, Research Center Borstel, Leibniz Center for Medicine and Biosciences, Borstel, Germany

ORCID IDs: 0000-0003-1422-5158 (R.B.); 0000-0001-8525-4939 (M.K.); 0000-0001-6094-7392 (J.D.A.); 0000-0002-3062-459X (B.W.).

Abstract

The signaling pathways that sustain the disease process of chronic rhinosinusitis with nasal polyps (CRSwNP) remain poorly understood. We sought to determine the expression levels of Wnt signaling genes in CRSwNP and to study the role of the Wnt pathway in inflammation and epithelial remodeling in the nasal mucosa. Microarrays and real time–quantitative polymerase chain reaction comparing gene expression in matched NPs and inferior turbinates revealed that *WNT2B*, *WNT3A*, *WNT4*, *WNT7A*, *WNT7B*, and *FZD2* were up-regulated and that *FZD1*, *LRP5*, *LRP6*, and *WIF1* were down-regulated in NPs. Immunolabeling showed robust expression of Wnt ligands, nuclear β-catenin, and Axin-2 in NP tissue, suggesting that Wnt/β-catenin signaling is activated in NPs. We used primary human nasal epithelial cell (HNEpC) cultures to test the functional consequences of Wnt pathway activation. Monolayer HNEpCs treated with recombinant human WNT (rhWNT) 3A, but not with rhWNT4, had altered epithelial morphology and decreased adhesion, without loss of viability. We found that neither rhWNT3A nor rhWNT4 treatment induced proliferation. The expression and release of inflammatory cytokines IL-6 and granulocyte-macrophage colony-stimulating factor were increased after rhWNT3A exposure of HNEpCs. When differentiated at an air–liquid interface, rhWNT3A- and WNT agonist–, but not rhWNT4-treated HNEpCs, had abnormal epithelial architecture, failed to undergo motile ciliogenesis, and had defective noncanonical Wnt (planar cell polarity) signaling. On the basis of these results, we propose a model in which Wnt/β-catenin signaling sustains mucosal inflammation and leads to a spectrum of changes consistent with those seen during epithelial remodeling in NPs.

Keywords: chronic rhinosinusitis with nasal polyps; Wnt; planar cell polarity; respiratory cilia; epithelial remodeling

Clinical Relevance

Chronic rhinosinusitis with nasal polyps is a common inflammatory condition of the nasal sinuses with substantial patient burden. Current disease models suggest that impaired local defense mechanisms, bacterial colonization, and disruption of the airway epithelial barrier set the stage for a self-perpetuating process of cyclical inflammation and tissue remodeling in the nasal mucosa. We show that canonical Wnt signaling is up-regulated in chronic rhinosinusitis with nasal polyps and that activation of canonical Wnt signaling in nasal epithelial cell cultures leads to cytokine release and a spectrum of changes consistent with those seen during epithelial remodeling of the nasal mucosa.

(Received in original form January 18, 2016; accepted in final form December 28, 2016)

*These authors contributed equally to this work.

This work was supported by University of Lübeck grant E38–2010, German Research Foundation grant BO 4143/1–1 (R.B.), and National Institutes of Health grant R01 GM098582 (J.D.A.).

Author Contributions: Conception and design: R.B. and E.K.V.; acquisition of data: R.B., E.K.V., M.K., B.H., and R.L.; analysis and interpretation: R.B., E.K.V., M.K., R.P., and N.R.; drafting and review of the manuscript for important intellectual content: R.B., E.K.V., M.K., N.R., J.D.A., J.V.N., and B.W. All authors gave final approval of the version to be published.

Correspondence and requests for reprints should be addressed to Robert Böscke, M.D, Department of Otolaryngology, Head and Neck Surgery, University Medical Center Schleswig-Holstein, Campus Lübeck, Ratzeburger Allee 160, 23538 Lübeck, Germany. E-mail: robert.boescke@gmail.com

This article has an online supplement, which is accessible from this issue's table of contents at www.atsjournals.org

Am J Respir Cell Mol Biol Vol 56, Iss 5, pp 575–584, May 2017

Originally Published in Press as DOI: 10.1165/rcmb.2016-0024OC on January 6, 2017
Internet address: www.atsjournals.org

Chronic rhinosinusitis (CRS) with nasal polyps (NPs) (CRSwNP) is considered a subgroup of CRS, a common inflammatory condition of the nasal and paranasal sinuses. CRSwNP is characterized by outgrowths from the nasal cavity mucosal lining, typically originating within the ethmoid sinuses (1, 2). Cardinal symptoms of CRS include chronic nasal congestion, nasal discharge, facial pressure, and hyposmia. Patients suffering from CRSwNP can benefit from topical and oral steroids, as well as from functional endoscopic sinus surgery, but even with the highest current standard of medical care and surgical treatments, the recurrence of upper airway inflammation and nasal polyposis remains high. Current CRSwNP disease models postulate that impaired local defense mechanisms, bacterial colonization, and disruption of the airway epithelial barrier (3) set the stage for a self-perpetuating process of cyclical inflammation and tissue remodeling in the nasal mucosa (1, 4, 5).

The signaling pathways that initiate and sustain the CRSwNP disease process remain elusive. In recent years, several pathways that are involved in embryonic lung development, such as Hedgehog and Wnt signaling, were found to become reexpressed in adult inflammatory and fibrotic lung diseases (6–12). These studies complement an increasing body of evidence for a role for Wnt signaling in injury repair (13) and inflammation (10, 14–16). The mammalian Wnt pathway is composed of a family of evolutionarily highly conserved genes, including 19 WNT glycoprotein ligands and 10 frizzled (FZD) transmembrane receptors. Wnt signaling involves at least three distinct, but overlapping, signal transduction pathways: canonical Wnt/β-catenin signaling, and the noncanonical Wnt/planar cell polarity (PCP) and Wnt/Ca^{2+} pathways (17). Canonical WNT ligands act as positive regulators by binding to FZD receptors/Lrp-5/6 coreceptors, leading to the inhibition of β-catenin degradation. β-Catenin stabilization in the cytoplasm leads to nuclear accumulation of β-catenin in a complex with the transcription factor transcription factor 1/lymphoid enhancer-binding factor 1 to regulate target gene expression (18). Although the pool of β-catenin that participates in signaling has a half-life of minutes, a highly stable form of β-catenin bound to the cytoplasmic tail of various cadherins localizes to epithelial adherens junctions (19). Noncanonical Wnt/PCP signaling regulates polarized cell morphologies, division, and migration and, in the respiratory system, it is required for axis elongation, lung branching morphogenesis, and the alignment of motile cilia for mucociliary clearance (20, 21). Directional information is communicated between cells by asymmetrically localized apical junctional complexes, which include FZD proteins and the Van Gogh-like 1 (VANGL1) family of PCP proteins (20).

Here, we show that Wnt signaling is up-regulated in NPs of CRSwNP nasal mucosa and that activation of canonical Wnt signaling in human nasal epithelial cells (HNEpCs) *in vitro* triggers cytokine release. In addition, canonical Wnt pathway activation leads to a spectrum of changes in HNEpCs that are consistent with those seen during tissue remodeling in NPs, including the loss of cellular differentiation and an abnormal epithelial morphology. We propose that Wnt pathway activation contributes to sustaining the inflammatory milieu and tissue remodeling in CRSwNP and that targeting this pathway may have future value in the treatment of patients with CRSwNP.

Materials and Methods

Study Subjects

NP and inferior turbinate (IT) tissues were harvested during sinus surgery at the Department of Otolaryngology, Head and Neck Surgery, University Medical Center Lübeck, Germany (microarray and real time–quantitative polymerase chain reaction [PCR]) or Stanford University Medical Center, Stanford, CA, (immunohistochemistry and cell culture). (*See* Table E1 in the online supplement for patient characteristics.) The study was approved by the human ethics committees of the University of Lübeck (AZ 10-201) and Stanford University School of Medicine (IRB-18981). All patients provided signed informed consent.

Microarray Analysis and Real Time–Quantitative PCR

NPs and ITs were harvested from the same patients ($n = 8$). Agilent whole human genome oligo microarrays 4 × 44K V1 were performed following the manufacturer's recommendations. Data analysis was performed using R software version 3.2.4. *P* values (two-tailed, unpaired *t* test with unequal variance) were corrected for multiple hypotheses testing using the Benjamini–Hochberg algorithm (false discovery rate determination) (22, 23). RNA was extracted using the RNeasy Mini Kit (QIAGEN, Hilden, Germany) and was reverse transcribed using the RevertAid First Strand cDNA Synthesis Kit (Fermentas, St. Leon-Rot, Germany). Real time–quantitative PCR reactions were performed using TaqMan Gene Expression Assays (Applied Biosystems, Foster City, CA) in a LightCycler 1.5 (Roche, Basel, Switzerland). Gene expression levels were normalized to *ACTB*, and relative changes were determined using the $2^{-\Delta\Delta Ct}$ method.

Immunohistochemistry

Tissues were fixed in 4% paraformaldehyde, infiltrated with 30% sucrose, cryoembedded in optimal cutting temperature compound (Thermo Fisher Scientific, Waltham, MA), and cryosectioned. Cell cultures were fixed in −20 °C methanol. Samples were incubated with primary antibodies (*see* online supplement) for 1 hour and with Alexa-fluor–conjugated secondary antibodies (Thermo Fisher Scientific) for 30 minutes, then visualized with a Leica TCS SP5 or SP8 confocal microscope (Leica Microsytems, Wetzlar, Germany). Relative signal intensity was calculated by normalizing NP values to the mean intensity of normal ITs measured using the Mean Gray Value function of the ImageJ software (National Institutes of Health).

HNEpC Cultures and Wnt Pathway Modulation

Healthy HNEpCs used for primary culture were obtained by protease digestion from ITs of patients undergoing turbinate reduction. For monolayer cultures, cells were seeded onto collagen-coated cell culture plates and grown in bronchial epithelial cell growth medium (Lonza, Basel, Switzerland). Cells were allowed to attach for 48 hours, then were exposed to recombinant human WNT (rhWNT) 3A or rhWNT4 (both 400 ng/ml; R&D Systems, Minneapolis, MN) for 6 to 96 hours, depending on the individual experiment.

Air–liquid interface (ALI) HNEpC cultures were grown using a modified mouse tracheal epithelial cell protocol (24). In short, cells were seeded onto collagen-coated Transwell inserts (Corning, Corning, NY) and cultured in proliferation medium (24) until confluency (approximately 5 days). ALI was created on confluency by adding differentiation medium (24) to the lower culture chamber only. ALI HNEpCs are fully mature from culture day ALI + 21. Cells were treated with rhWNT3A (200 or

400 ng/ml; R&D Systems), rhWNT4 (200 or 400 ng/ml, R&D Systems or Abnova, Taipei, Taiwan) or 1.5 or 3 μM CHIR99021 (Axon Medchem, Groningen, the Netherlands) for 10 days from culture day ALI + 0 or ALI + 30.

Statistical Analysis

Experiments were performed in triplicate at $n \geq 3$. Results are presented as mean ± SEM or SD and were considered statistically significant at $P < 0.05$. Means were compared using a two-tailed Student's *t* test (real time–quantitative PCR, cytometric bead array, and 3-[4,5-dimethylthiazol-2-yl]-2,5-diphenyl tetrazolium bromide assays and immunohistochemistry) or a one-sample *t* test (real-time cell analysis [RTCA] assay). Graphs were generated using the GraphPad Prism Software 7.0 (GraphPad Software, La Jolla, CA).

For detailed methodology, *see* the online supplement.

Results

Microarray analysis of NP and IT tissues revealed differential gene expression of Wnt pathway genes (Figure E1 and Table E2). Several WNT ligands were significantly up-regulated in NP compared with IT tissue: *WNT3A*, 3.16-fold ($P = 0.038$); *WNT4*, 6-fold ($P = 0.003$); *WNT7A*, 4.22-fold ($P = 0.006$); and *WNT7B*, 2.53-fold ($P = 0.016$). None of the Wnt ligands were down-regulated significantly in NPs. Analysis of WNT receptor genes revealed statistically significant up-regulation of *FZD2* (2.62-fold; $P = 0.029$) and down-regulation of *FZD1* (−1.61-fold; $P = 0.03$), *LRP5* (−1.7-fold; $P = 0.017$), and *LRP6* (−1.86-fold; $P = 0.003$). Furthermore, we found down-regulation of the Wnt inhibitor *WIF1* (−4.69-fold; $P = 0.054$) and differential expression of several target genes of Wnt/β-catenin signaling, such as *WISP1* (4.47-fold; $P < 0.001$) (Table E3).

To validate the microarray analysis results, we performed real time–quantitative PCR for selected Wnt pathway molecules (Figure 1). Real time–quantitative PCR results revealed significant expression differences for NPs versus ITs for *WNT2B* (1.82-fold ± 1.163 [SEM]); $P = 0.005$), *WNT3A* (3.27-fold ± 1.28; $P = 0.002$), *WNT4* (5.15-fold ± 1.25; $P < 0.001$), *WNT7A* (2.67-fold ± 1.34; $P = 0.01$), *WNT7B* (2.33-fold ± 1.32; $P = 0.02$), *FZD2* (2.84-fold ± 1.29; $P = 0.005$), *FZD4* (−1.70-fold ± 1.28; $P = 0.04$), *FZD7* (−1.89-fold ± 1.28; $P = 0.03$), *LRP5* (−1.72-fold ± 1.25; $P = 0.04$), *LRP6* (−2.04-fold ± 1.33; $P = 0.04$), *WIF1* (−12.82-fold ± 2.683; $P = 0.04$), and *WISP1* (4.91-fold ± 1.39; $P = 0.002$). Real time–quantitative PCR did not reveal statistically significant down-regulation of *FZD1* (−1.47-fold ± 1.20; $P = 0.07$). Neither microarray nor real time–quantitative PCR showed significant changes in the noncanonical Wnt ligand *WNT5A* (1.23-fold, $P = 0.80$ for microarray; 1.40-fold ± 1.27, $P = 0.20$ for real time–quantitative PCR). Thus, our results indicate that multiple Wnt signaling components are enriched in NPs, suggesting that this pathway may be involved in NP pathogenesis.

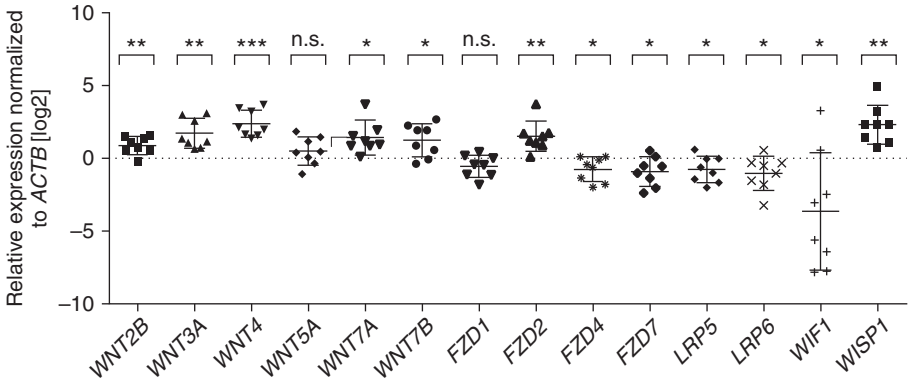

Figure 1. Validation of nasal polyp (NP) and inferior turbinate (IT) microarray results by real time–quantitative polymerase chain reaction (PCR) for selected Wnt pathway components. Real time–quantitative PCR results revealed significant expression differences between NPs and ITs for *WNT2B, WNT3A, WNT4, WNT7A, WNT7B, FZD2, FZD4, FZD7, LRP5, LRP6, WIF1*, and *WISP1,* but not for *WNT5A* or *FZD1*. Real time–quantitative PCRs were performed in triplicate on $n = 8$ matched NPs and corresponding ITs from the same donor. Log2-scale. *Bar graphs* represent the mean ± SD. n.s., not significant. $^{*}P < 0.05$, $^{**}P < 0.01$, $^{***}P < 0.001$ (two-tailed Student's *t* test).

It is accepted that Wnt ligands can act through a β-catenin–dependent (canonical) or –independent (noncanonical) downstream signaling cascade, although some overlap exists between the two processes, and many regulatory aspects remain elusive (17, 19). Because our results suggest that the Wnt pathway is active in NPs, we tested whether this is accompanied by changes in β-catenin localization, abundance, and phosphorylation state. Normal IT tissue from three different donors (one shown in Figure 2A) showed robust labeling of only the apical epithelial junctions (marked by E-cadherin) with nonphosphorylated β-catenin antibody consistent with cadherin-bound β-catenin found in intact epithelia (18). Normal ITs had no detectable phospho-Tyr489–β-catenin, an active form of β-catenin (25, 26) (Figure 2A). In contrast, NP samples from eight different donors showed abundant signal for phospho-Tyr489–β-catenin in the epithelium (12.01-fold ± 1.14, $P < 0.0001$) and the submucosal/lamina propria (18.73-fold ± 1.61, $P < 0.0001$) regions (Figure 2A). Higher magnification NP images (Figure 2B) demonstrate that phospho-Tyr489–β-catenin is nuclear in some cells (boxed areas), and that it can also be found in infiltrating lymphocytes detected with the CD45 pan-lymphocyte marker. NPs still showed nonphosphorylated β-catenin antibody labeling in both epithelial and submucosal regions (Figure 2A); however, the junctional signal was often reduced or discontinuous, likely because of the abnormal epithelial architecture of NP tissues. To further validate Wnt/β-catenin activity, we performed immunolabeling for anti-Axin-2 (27), a direct target of the Wnt pathway via transcription factor 1/lymphoid enhancer-binding factor 1 transcription factors that participates in a negative feedback loop in Wnt/β-catenin signaling. We detected robust labeling for anti-Axin-2 in all NP samples compared with normal ITs in both the epithelium (10.66-fold ± 4.46, $P = 0.002$) and the NP interior (20.93-fold ± 2.58, $P < 0.0001$) (Figure E3). Collectively, our results indicate that canonical Wnt/β-catenin signaling is activated in NPs.

To dissect the role of Wnt signaling in NPs, we focused on WNT3A, the most well-known activator of canonical Wnt signaling, and WNT4, the most highly NP-enriched WNT ligand in our dataset.

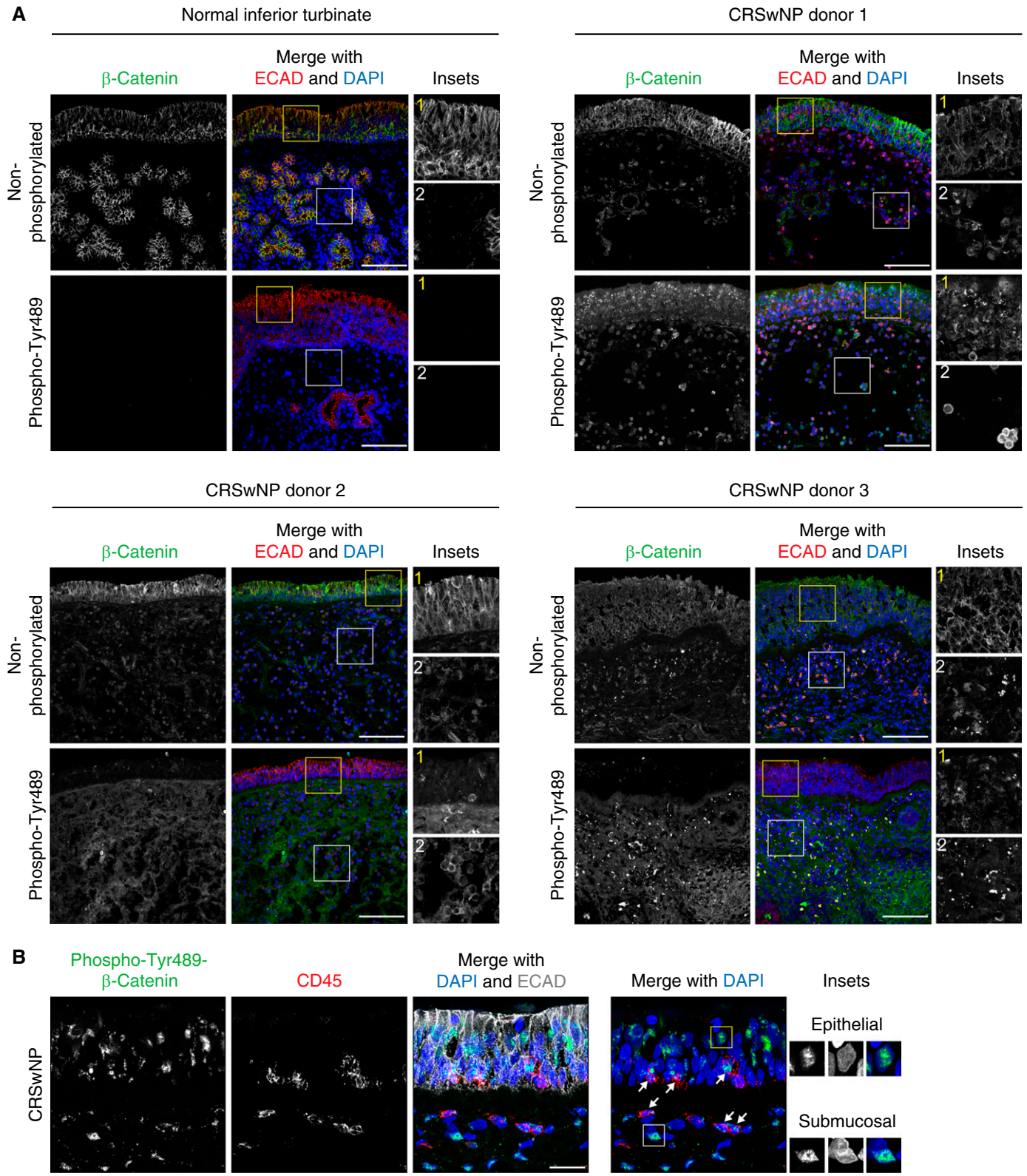

Figure 2. β-Catenin expression in normal IT and NP tissues. (*A*) Normal IT and NP cryosections (from three donors) were labeled with non-phospho–β-catenin (*top*) or phospho-Tyr489–β-catenin (*bottom*) (*green*) and E-cadherin (ECAD, *red*) antibodies and DAPI (*blue*). Normal ITs showed strong epithelial junctional labeling for non-phospho–β-catenin and no signal for phospho-Tyr489–β-catenin. NPs showed epithelial junctional labeling and signal in the NP interior for non-phospho–β-catenin and strong epithelial and submucosal labeling for phospho-Tyr489–β-catenin. Insets show a higher

WNT4 has been known to regulate both canonical and noncanonical Wnt signaling (28). Consistent with our finding of up-regulated WNT gene expression, we found significantly stronger immunohistochemical labeling with anti-WNT3A and WNT4 antibodies in NPs from three donors in both the mucosal epithelium (3.38-fold ± 0.23, $P < 0.0001$, and 1.44-fold ± 0.14, $P = 0.0006$) and the submucosal region (5.88-fold ± 0.56, $P < 0.0001$, and 2.05-fold ± 0.23, $P < 0.0001$) of NPs (Figure 3A) compared with ITs from three donors (Figure 3B). WNT2, which showed modestly up-regulated gene expression in NPs, also showed strong labeling in NP tissue (Figure E2), but we did not pursue this finding any further. Thus, we identified WNT3A and WNT4 as candidates for Wnt pathway regulation in NP pathogenesis.

Because previous studies of airway epithelia indicated that Wnt signaling drives inflammation (8, 10), we tested the release of proinflammatory mediators from primary monolayer HNEpC cultures derived from normal donor tissue after rhWNT treatment. Cytometric bead array analysis revealed that exogenous rhWNT3A led to significantly increased secretion of IL-6 (2.27 ± 0.33; $P = 0.009$) and granulocyte-macrophage colony-stimulating factor (GM-CSF) (2.1 ± 0.5; $P = 0.02$) from HNEpCs 24 hours after stimulation. Secretion of IL-8 was not altered significantly (1.25 ± 0.033; $P = 0.14$). Exogenous rhWNT4 did not significantly alter the release of IL-6 (1.23 ± 0.068; $P = 0.08$), GM-CSF (1.2 ± 0.15; $P = 0.16$), and IL-8 (1.08 ± 0.08; $P = 0.28$) into the culture supernatant (Figure 4A). Although rhWNT3A stimulation induced cytokine release, we did not detect a statistically significant corresponding increase in gene expression by real time–quantitative PCR (*IL6* [1.54 ± 0.24; $P = 0.59$], *IL8* [0.93 ± 0.12; $P = 0.26$], and *GMCSF* [2.18 ± 0.47; $P = 0.11$]) (Figure 4B). rhWNT4 treatment of HNEpC cultures also had no effect on cytokine gene expression (*IL6* [1.00 ± 0.25; $P = 0.59$], *IL8* [0.93 ± 0.11; $P = 0.26$], and *GM-CSF* [1.06 ± 0.12; $P = 0.11$]) (Figure 4B). These results indicate that WNT3A, but not WNT4, induces the release of cytokines in HNEpCs. We postulate that this occurs through the activation of Wnt/β-catenin signaling, which thus may be a potential driver of inflammation in the nasal mucosa during NP pathogenesis.

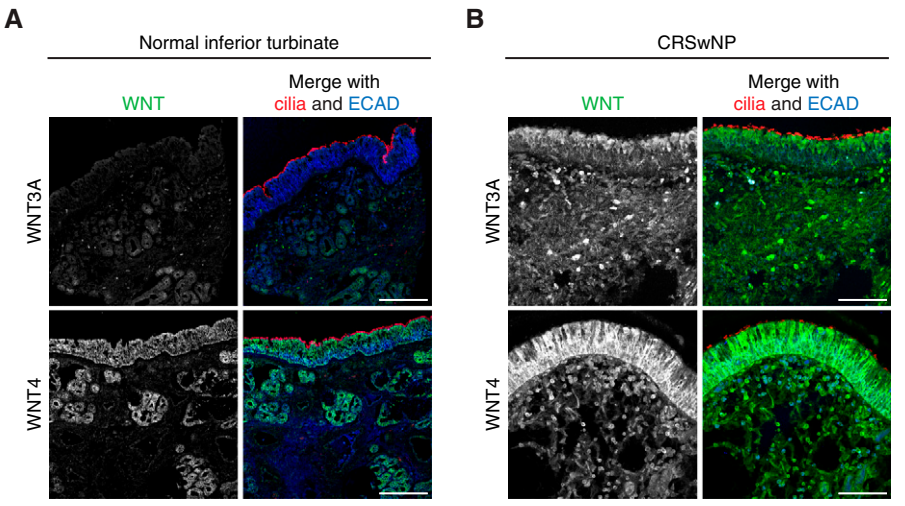

Figure 3. Wnt expression in normal IT and NP tissues. (*A*) Normal IT tissue cryosections labeled with WNT3A (*top*) or WNT4 (*bottom*) (*green*), acetylated α-tubulin (cilia, *red*), and ECAD (*blue*) antibodies show weak anti-WNT3A and moderate anti-WNT4 antibody labeling. WNT4 was localized mainly in the mucosal and glandular epithelia of the IT. (*B*) NP cryosections labeled with WNT3A (*top*) or WNT4 (*bottom*) (*green*), acetylated α-tubulin (cilia, *red*), and ECAD (*blue*) antibodies show strong anti-WNT3A and anti-WNT4 antibody labeling in the mucosal epithelium and in cells scattered in the NP interior. Images are representative of $n = 8$ NP and $n = 3$ normal IT samples. *Scale bars*: 100 μm.

A major component in the pathogenesis of NPs is cellular proliferation that leads to NP enlargement and consequent upper airway obstruction. Because Wnt signaling promotes proliferation in both development and disease (29, 30), we next tested for a proliferative effect of rhWNT proteins on monolayer cultures of primary HNEpCs by continuously monitoring rhWNT3A- or rhWNT4-treated cultures in an RTCA system. Unexpectedly, RTCA results of rhWNT3A-treated HNEpCs showed a gradual decline in the normalized impedance curve/cell index (CI) beginning ~30 hours after treatment, whereas the CI curve for rhWNT4-treated HNEpCs was not significantly different from that of untreated HNEpCs (Figures 5 and E4). Declining CI levels indicate a decrease in adherence of cells to the culture plate, which can be caused by the dispersion of cells, cellular morphological changes, or the detachment of cells because of cell death. To test for loss of HNEpC viability after rhWNT3A treatment, we performed the 3-[4,5-dimethylthiazol-2-yl]-2,5-diphenyl tetrazolium bromide assay that detects cytotoxicity by indirectly measuring the activity of mitochondrial dehydrogenases. We did not find significant differences between untreated and rhWNT3A-treated HNEpCs after 24, 48, 72, and 96 hours of treatment (Figure E5). Thus, we interpreted the RTCA CI decline after rhWNT3A exposure to be a measure of cellular morphological and/or behavioral changes.

On the basis of these results, we further explored the role of Wnt signaling using a primary ALI HNEpC culture system. ALI HNEpCs are initiated from basal stem cells isolated from healthy donor tissue, which initially proliferate when submerged in media and then are allowed

Figure 2. (Continued). magnification view of the epithelial (*yellow boxes*) and the submucosal (*white boxes*) β-catenin signal. Submucosal ECAD signal in NPs derives from infiltrating lymphocytes. (*B*) NP cryosections labeled with phospho-Tyr489–β-catenin (*green*), CD45 (*red*), and ECAD (*gray*) antibodies and DAPI (*blue*) show that NPs contain $CD45^+$ lymphocytes, some of which are phospho-Tyr489–β-catenin–positive (*arrows*). Insets show nuclear localization for phospho-Tyr489–β-catenin in the epithelial (*yellow box*) and the submucosal (*white box*) regions. Images are representative of $n = 8$ NP and $n = 3$ normal IT samples. *Scale bars*: 100 μm (*A*); 25 μm (*B*). CRSwNP, chronic rhinosinusitis with nasal polyps.

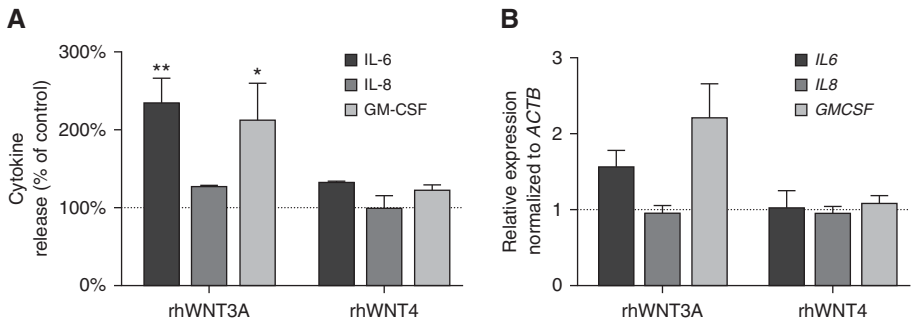

Figure 4. Proinflammatory cytokine expression and release in recombinant human WNT (rhWNT) 3A- and rhWNT4-treated monolayer human nasal epithelial cell (HNEpC) cultures. (*A*) Cytometric bead arrays (CBA) of HNEpC supernatants revealed significantly increased IL-6 and granulocyte-macrophage colony-stimulating factor (GM-CSF) release after rhWNT3A (400 ng/ml for 24 h) stimulation, but not after rhWNT4 (400 ng/ml for 24 h) treatment. IL-8 release was not altered significantly in either rhWNT3A- or rhWNT4-treated supernatants. *Dotted line* indicates baseline cytokine release of unstimulated control. Data from $n = 3$ CBA experiments are shown. $^{*}P < 0.05$, $^{**}P < 0.01$ (Student's two-tailed t test). (*B*) Real time–quantitative PCR analysis of cytokine expression in rhWNT3A- and rhWNT4-treated (both 400 ng/ml for 6 h) monolayer HNEpCs failed to demonstrate a statistically significant difference compared with untreated cells for *IL6*, *IL8*, and *GMCSF* (Student's two-tailed t test). Data from $n = 5$ representative experiments are shown. *Bar graphs* represent the mean ± SEM.

to differentiate on a porous membrane surface under ALI conditions (31). ALI culture supports the differentiation of a complex epithelial layer with multiciliated and secretory cell types, which faithfully models the *in vivo* pseudostratified airway epithelium. We exposed undifferentiated (ALI + 0 days) and fully differentiated (ALI + 30 days) ALI HNEpCs to rhWNT3A, rhWNT4, or the canonical Wnt agonist (glycogen synthase kinase 3 inhibitor) CHIR99021 for 10 days of ALI culture. Untreated and rhWNT4-treated ALI + 0 day cultures matured into multiciliated epithelia (cilia are marked by acetylated α-tubulin antibody labeling; the fraction of multiciliated cells is 0.35 ± 0.02 at ALI + 10 days in untreated cultures) with approximately uniform apical cell size, a mostly hexagonal apical cell surface shape, and robust adherens junctions as indicated by E-cadherin antibody labeling (Figure E6; rhWNT4 from two different manufacturers was tested to confirm results, not shown). In contrast, multiciliated cells failed to emerge in ALI + 0 day cultures treated with rhWNT3A (fraction of multiciliated cells, 0.07 ± 0.03; $P < 0.0001$) or CHIR99021 (0.02 ± 0.01; $P < 0.0001$) for 10 days (Figure 6A). Furthermore, E-cadherin localization was decreased and discontinuous at the apical junctions and accumulated in the cytoplasm. The apical surface size and shape were notably irregular, and many cells adopted a flattened and highly elongated morphology. Cell shape changes can be demonstrated by calculating the ratio of the long versus short axis of cells on the basis of the E-cadherin signal, which shows that untreated cultures have a long versus short axis ratio of 1.35 ± 0.05 in contrast to rhWNT3A- and CHIR99021-treated cells with ratios of 3.73 ± 0.32 ($P < 0.0001$) and 3.49 ± 0.22 ($P < 0.0001$), respectively. These alterations are reminiscent of epithelial to mesenchymal transformation (EMT), a continuum of pathogenic cellular changes linked to airway diseases with epithelial remodeling (11, 32–34). Although we did not detect a complete EMT response as marked by the expression of α-smooth muscle actin (not shown), Wnt pathway activation may propel cells along the EMT continuum from a normal epithelial morphology toward abnormal mucosal architecture.

Loss of normal apical morphology on rhWNT3A and CHIR99021 treatment points toward compromised cell polarity. Because the orientation of cilia, the integrity of apical cell junctions, and the regenerative capacity of respiratory epithelia are specified by the noncanonical Wnt/PCP signaling (21, 35), we analyzed the localization of the PCP protein VANGL1, which reports on Wnt/PCP pathway activity. In untreated and rhWNT4-treated undifferentiated (ALI + 0 day) cultures, VANGL1 showed the characteristic asymmetric distribution pattern at the apical adherens junctions (Figures 6A and E6; VANGL1 asymmetry is quantified by the Manders' coefficient of overlap for the VANGL1 and E-cadherin channels of the same image [*see* Materials and Methods]; 0.57 ± 0.02 in untreated cultures), whereas cultures treated with rhWNT3A (0.91 ± 0.01; $P < 0.0001$) and CHIR99021 (0.96 ± 0.01; $P < 0.0001$) showed uniform junctional distribution of VANGL1. Our results suggest that ectopic canonical Wnt pathway activation also blocks PCP signaling in HNEpCs. We demonstrated that the constellation of phenotypic changes in CHIR99021- and rhWNT3A-treated ALI HNEpCs is dose dependent (Figure E7). Loss of VANGL1 asymmetric localization and multiciliated cell differentiation were readily observed at lower doses of CHIR99021 and rhWNT3A, but higher doses were required to elicit cell shape changes.

Interestingly, the alterations induced by rhWNT3A and CHIR99021 in undifferentiated ALI HNEpC cultures could not be triggered in fully differentiated (ALI + 30 day) cultures (Figure 6B). rhWNT4 treatment likewise had no effect on fully differentiated cultures (Figure E6). Because ALI cultures are initiated using basal stem cells isolated from adult epithelia, ALI + 0 day cultures most accurately model the regenerating airway epithelium, whereas ALI + 30 day cultures represent the intact, mature respiratory epithelium. These data indicate that Wnt activation alone is not sufficient to trigger NP-like changes in intact, differentiated epithelia, and suggest that prior event(s) leading to epithelial injury are required.

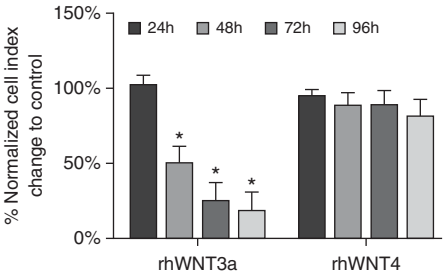

Figure 5. Real-time cell analysis (RTCA) of rhWNT3A- and rhWNT4-stimulated monolayer HNEpC cultures. *Bar graphs* represent the normalized RTCA cell index change of HNEpCs stimulated with rhWNT3A or rhWNT4 (both 400 ng/ml) for 96 hours relative to corresponding unstimulated controls. Data are representative of $n = 3$ experiments. $^{*}P < 0.05$ (one-sample t test). *Bar graphs* represent the mean ± SEM.

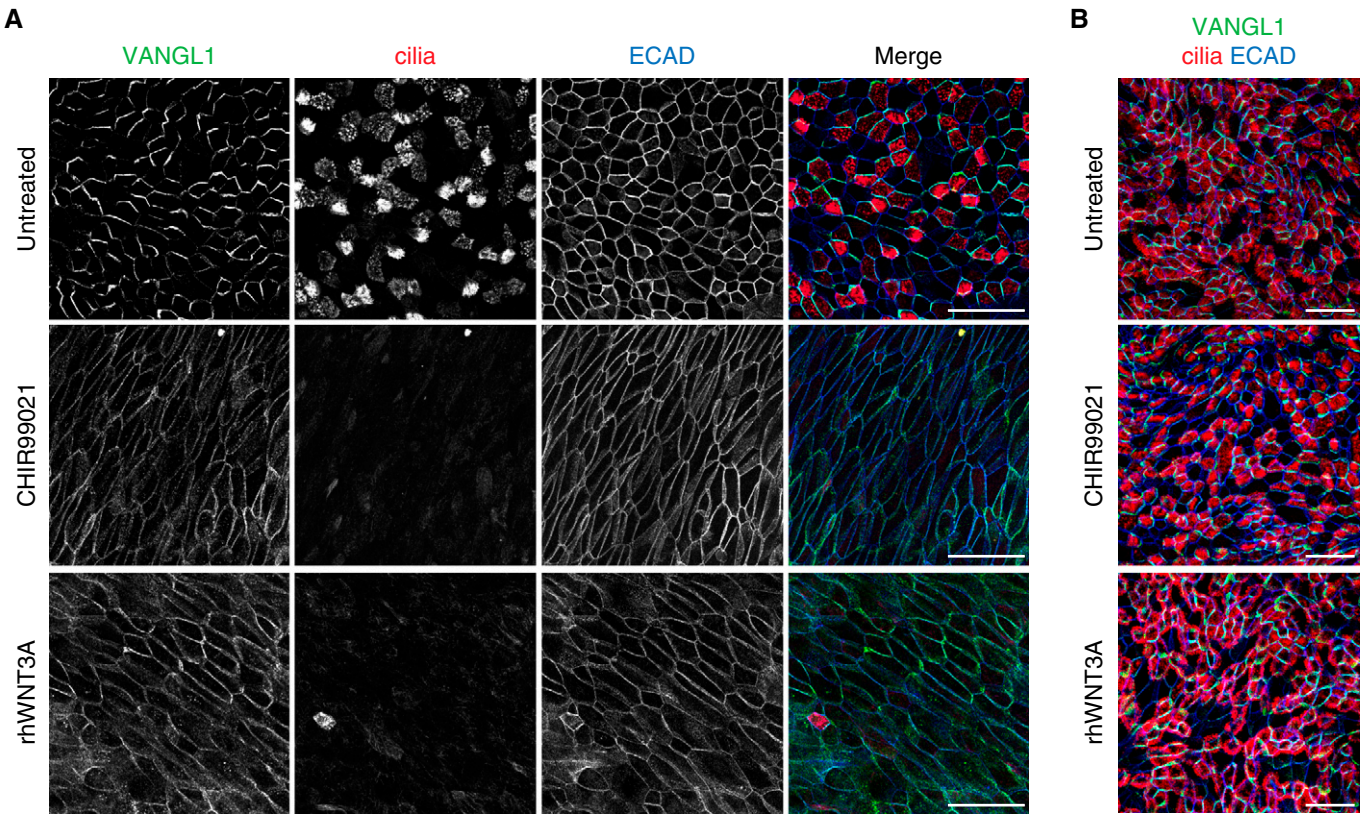

Figure 6. rhWNT3A treatment induces motile ciliogenesis and epithelial junctional and planar cell polarity signaling defects in air–liquid interface (ALI) HNEpC cultures. (*A*) Undifferentiated ALI HNEpC cultures were treated with 3 μM CHIR99021 or 400 ng/ml rhWNT3A for 10 days, then labeled with Van Gogh–like 1 (VANGL1), acetylated α-tubulin (cilia, *red*), and ECAD (*blue*) antibodies. After 10 days of *in vitro* differentiation, untreated cultures showed asymmetric apical junctional VANGL1 signal, robust motile ciliogenesis, uniform cell shape and size, and intact adherens junctions (ECAD). CHIR99021- and rhWNT3A-treated cultures lacked VANGL1 asymmetric localization; multiciliated cells failed to emerge and had elongated cell shapes with uneven ECAD labeling. (*B*) Fully differentiated ALI HNEpC cultures were treated with 3 μM CHIR99021 or 400 ng/ml rhWNT3A for 10 days, then labeled with VANGL1, acetylated α-tubulin (cilia, *red*), and ECAD (*blue*) antibodies. CHIR99021 and rhWNT3A treatment had no effect on VANGL1 localization, multiciliated cells, cell shape, or apical junctions. Images are representative of $n \geq 3$ drug treatments of ALI HNEpCs generated from $n = 3$ healthy donors. *Scale bars*: 50 μm (*A* and *B*).

In sum, we show that Wnt signaling is active in NPs and that canonical Wnt pathway activation in HNEpCs, mediated, at least in part, by WNT3A, leads to structural and functional alterations, including proinflammatory cytokine release and loss of normal cellular morphology, polarization, and differentiation, which are consistent with changes seen during tissue remodeling in NPs and other airway diseases.

Discussion

The cellular signaling pathways that govern the pathological hallmarks of CRSwNP (inflammation and tissue remodeling) remain poorly understood. Existing models of CRSwNP propose that inflammation and tissue remodeling arise from structural and functional damage of the epithelial barrier (36–39), but the molecular changes that accompany these events and those that drive NP evolution are not well known.

We sought to define the expression profile of Wnt pathway molecules in CRSwNP disease and to elucidate their roles in epithelial barrier function, tissue remodeling, and inflammation. We demonstrate altered gene expression consistent with Wnt pathway activation in NPs and provide evidence from primary cell culture studies that this leads to epithelial dysfunction and proinflammatory cytokine release. On the basis of our results, we propose the following model for pathogenic Wnt signaling in CRSwNP: (*1*) Wnt signaling is up-regulated in NPs downstream of prerequisite inciting events such as epithelial damage, infection, and/or inflammation; (*2*) Wnt signaling exacerbates epithelial barrier dysfunction and compromised mucociliary clearance by blocking the formation of a normal multiciliated epithelium, contributing to epithelial remodeling; and (*3*) Wnt signaling sustains and potentiates inflammation via proinflammatory cytokine release in the upper airway epithelium.

There is ample evidence that both canonical (or β-catenin–dependent) and noncanonical Wnt pathways are essential for the proper development and maintenance of the airways (40–42) and that they are misregulated in a variety of disease conditions (12). Here, we show that NPs are positive for phospho-Tyr489–β-catenin, an active form of β-catenin, as well as Axin-2 which suggests that canonical Wnt signaling operates in NPs. We also demonstrate that WNT3A, the prototypical canonical Wnt ligand, is highly expressed in NPs. However, we found that, unlike in other systems (9, 10, 40, 43–45), it did

not promote epithelial cell proliferation as a potential mechanism for NP formation, although we cannot rule out such effects on the submucosal cell population. Instead, we found evidence for WNT3A driving a variety of epithelial morphological and functional changes that may contribute to NP pathogenesis. Future studies will be required to elucidate the signaling mechanism that connects Wnt binding to these cellular changes. Furthermore, we also detected the enrichment of other Wnt ligands in NPs, some of which are implicated in noncanonical pathways. We also explored the role of WNT4, the most highly expressed Wnt ligand in NPs; however, we did not observe any of the changes elicited by rhWNT3 treatment in response to rhWNT4 from two different manufacturers. Nevertheless, WNT4 and other WNTs may still play important roles in NP formation through either canonical or noncanonical pathways. We also detected down-regulation of several Wnt pathway receptor genes in NPs, and we speculate that by analogy to autoregulatory negative feedback loops in other pathways (46) this may occur as a consequence of chronic Wnt pathway activation. Thus, we can positively link canonical Wnt signaling to NP pathogenesis but cannot rule out a more complicated set of events driven by multiple Wnt signaling cascades. This is supported by the Wnt/PCP (noncanonical) defects we observed in rhWNT3A-treated HNEpCs, which raises the possibility that crosstalk between Wnt pathways may be involved in NP pathogenesis.

To study the role of Wnt signaling in NPs, we leveraged the strength of well-characterized primary monolayer and ALI HNEpC culture systems and modeled canonical Wnt pathway activation by rhWNT3A or CHRI99021 treatment. We found that canonical Wnt pathway activation in normal HNEpCs induces proinflammatory cytokine release. Although previous studies have shown that Wnt signaling can elicit cytokine release (10, 13–16), we demonstrate that in rhWNT3A-treated HNEpCs, the release of proinflammatory cytokines, which are associated with CRS (1), also accompanies morphological changes in the epithelium.

The most notable of these changes was the loss of normal cell shape and apical junctional integrity in CHIR99021- and rhWNT3A-treated HNEpCs. Epithelial barrier defects caused by impaired cell–cell junctions (34, 39, 47) have been proposed as major drivers of NP pathogenesis because they allow pathogens to invade the underlying mucosal tissues and to trigger immune responses (48). We believe that canonical Wnt pathway activation in HNEpC elicits morphological changes similar to those observed in NPs *in vivo* (34, 39, 47), and that this occurs via defective apicobasal polarity and altered cell and epithelial patterning that disrupts the normal architecture of the airway epithelium. This model is supported by results from studies of transgenic mice expressing stabilized β-catenin, which blocked the differentiation of spatially appropriate airway epithelial cell types and resulted in the formation of polyp-like structures in the trachea and the dilation of the lower airways. In addition to the loss of apical-basal polarity, we found evidence that Wnt/PCP signaling was disrupted in CHIR99021- and rhWNT3A-treated HNEpC ALI cultures. PCP in the airway epithelium provides directional cues that guide the proper three-dimensional organization of the developing respiratory system, and also orient motile cilia for mucociliary clearance. Recently, it was also shown to be required for apical junctional integrity and regenerative capacity in the airway epithelium. In other tissues, PCP signaling controls cell migration and morphology, and we propose that defective PCP could contribute to the aberrant epithelial cell behaviors involved in generating NPs.

We also observe that Wnt activation in ALI HNEpCs blocked the differentiation of multiciliated cells. NPs may or may not possess cilia, but loss of cilia has been correlated with increased CRSwNP disease severity (47). Multiciliated cells can be lost because of infection or injury, and inflammation is known to shift the ratio of multiciliated and secretory cell types because of mucous cell hyperplasia (49). The loss of cilia impairs mucociliary clearance and likely other aspects of airway epithelial homeostasis, which raises the possibility that multiciliated cell defects contribute to CRSwNP disease.

Finally, we raise the possibility that Wnt activation is a downstream, rather than an inciting, event in NP formation. The finding that the structural and functional changes seen in undifferentiated rhWNT3A-treated ALI HNEpCs cultures could not be triggered in fully differentiated cultures implies that inappropriate activation of Wnt/β-catenin signaling can interfere with regenerating, but not intact, fully differentiated airway epithelia. From this, we infer that Wnt signaling activation in the *in vivo* nasal mucosa is not by itself sufficient to trigger pathological alterations in well-differentiated, undamaged airway epithelia. We suggest that preexisting chronic inflammation and injury of the nasal mucosa, giving rise to alerted cell–cell and/or cell–extracellular matrix interactions, is a prerequisite for Wnt to drive further pathological tissue remodeling and immune modulation involved in NP formation.

Our work was prompted by reports that implicated Wnt signaling in the pathogenesis of lower airway diseases such as idiopathic pulmonary fibrosis (7, 9, 50) and bronchial asthma (8), although these reports do not provide a clear mechanistic picture of Wnt function. Subtypes of CRSwNP and CRS without NPs share multiple pathological features with lower airway diseases, including epithelial damage, fibrosis/scar formation, and inflammation. Wnt/β-catenin pathway activation has been attributed to a variety of pathological events, such as inflammation, epithelial proliferation and differentiation, fibroblast migration, extracellular matrix deposition, and myofibroblast differentiation, in lower airway diseases (9, 10, 44). On the basis of the well-established comorbidity of Th2-skewed CRSwNP and eosinophilic asthma, it is noteworthy that "Th2-high" asthma has also been found to show increased expression of Wnt signaling molecules (8). In sum, we believe that although Wnt signaling is essential for the proper development of the respiratory system, including the differentiation of the epithelium, its aberrant activation is a key and frequent player in respiratory diseases featuring epithelial dysfunction.

Conclusions

In conclusion, we have demonstrated that the canonical Wnt pathway is activated in NPs and that *in vitro* Wnt activation in the context of the regenerating epithelium triggers cytokine release and leads to the formation of an abnormal epithelium with compromised adherens junctions, absent ciliogenesis, and impaired PCP signaling. We propose a model in which canonical Wnt signaling promotes epithelial dysfunction and remodeling after an

inciting event such as chronic infection and inflammation, leading to NP pathogenesis. Thus, modulation of Wnt signaling should be explored as a novel target for pharmacological intervention in the treatment of CRSwNP. ■

Author disclosures are available with the text of this article at www.atsjournals.org.

Acknowledgments: The authors thank Robert Durruthy-Durruthy (Stanford University) for help with the microarray data analysis. They also thank Alan Nguyen (Stanford University), Dawn Bravo (Stanford University), Shanel Tsuda (Stanford University), Brigitte Wollmann (University of Lübeck), and Silvia Grammerstorf-Rosche (University of Lübeck) for their support regarding several parts of this work.

References

1. Fokkens WJ, Lund VJ, Mullol J, Bachert C, Alobid I, Baroody F, Cohen N, Cervin A, Douglas R, Gevaert P, *et al*. European position paper on rhinosinusitis and nasal polyps 2012. *Rhinol Suppl* 2012:3, 1–298.
2. Rosenfeld RM, Piccirillo JF, Chandrasekhar SS, Brook I, Ashok Kumar K, Kramper M, Orlandi RR, Palmer JN, Patel ZM, Peters A, *et al*. Clinical practice guideline (update): adult sinusitis. *Otolaryngol Head Neck Surg* 2015; 152:S1–S39.
3. Zhang N, Van Crombruggen K, Gevaert E, Bachert C. Barrier function of the nasal mucosa in health and type-2 biased airway diseases. *Allergy* 2016;71:295–307.
4. Van Bruaene N, Bachert C. Tissue remodeling in chronic rhinosinusitis. *Curr Opin Allergy Clin Immunol* 2011;11:8–11.
5. Barham HP, Osborn JL, Snidvongs K, Mrad N, Sacks R, Harvey RJ. Remodeling changes of the upper airway with chronic rhinosinusitis. *Int Forum Allergy Rhinol* 2015;5:565–572.
6. Kugler MC, Joyner AL, Loomis CA, Munger JS. Sonic hedgehog signaling in the lung. From development to disease. *Am J Respir Cell Mol Biol* 2015;52:1–13.
7. Königshoff M, Balsara N, Pfaff EM, Kramer M, Chrobak I, Seeger W, Eickelberg O. Functional Wnt signaling is increased in idiopathic pulmonary fibrosis. *PLoS One* 2008;3:e2142.
8. Choy DF, Modrek B, Abbas AR, Kummerfeld S, Clark HF, Wu LC, Fedorowicz G, Modrusan Z, Fahy JV, Woodruff PG, *et al*. Gene expression patterns of Th2 inflammation and intercellular communication in asthmatic airways. *J Immunol* 2011;186: 1861–1869.
9. Chilosi M, Poletti V, Zamò A, Lestani M, Montagna L, Piccoli P, Pedron S, Bertaso M, Scarpa A, Murer B, *et al*. Aberrant Wnt/β-catenin pathway activation in idiopathic pulmonary fibrosis. *Am J Pathol* 2003; 162:1495–1502.
10. Aumiller V, Balsara N, Wilhelm J, Günther A, Königshoff M. WNT/β-catenin signaling induces IL-1β expression by alveolar epithelial cells in pulmonary fibrosis. *Am J Respir Cell Mol Biol* 2013;49:96–104.
11. Königshoff M, Kramer M, Balsara N, Wilhelm J, Amarie OV, Jahn A, Rose F, Fink L, Seeger W, Schaefer L, *et al*. WNT1-inducible signaling protein-1 mediates pulmonary fibrosis in mice and is upregulated in humans with idiopathic pulmonary fibrosis. *J Clin Invest* 2009;119:772–787.
12. Königshoff M, Eickelberg O. WNT signaling in lung disease: a failure or a regeneration signal? *Am J Respir Cell Mol Biol* 2010;42:21–31.
13. Whyte JL, Smith AA, Helms JA. Wnt signaling and injury repair. *Cold Spring Harb Perspect Biol* 2012;4:a008078.
14. Halleskog C, Mulder J, Dahlström J, Mackie K, Hortobágyi T, Tanila H, Kumar Puli L, Färber K, Harkany T, Schulte G. WNT signaling in activated microglia is proinflammatory. *Glia* 2011;59:119–131.
15. Sen M, Lauterbach K, El-Gabalawy H, Firestein GS, Corr M, Carson DA. Expression and function of wingless and frizzled homologs in rheumatoid arthritis. *Proc Natl Acad Sci USA* 2000;97:2791–2796.
16. Blumenthal A, Ehlers S, Lauber J, Buer J, Lange C, Goldmann T, Heine H, Brandt E, Reiling N. The Wingless homolog WNT5A and its receptor Frizzled-5 regulate inflammatory responses of human mononuclear cells induced by microbial stimulation. *Blood* 2006; 108:965–973.
17. Niehrs C. The complex world of WNT receptor signalling. *Nat Rev Mol Cell Biol* 2012;13:767–779.
18. Nelson WJ, Nusse R. Convergence of Wnt, β-catenin, and cadherin pathways. *Science* 2004;303:1483–1487.
19. Clevers H, Nusse R. Wnt/β-catenin signaling and disease. *Cell* 2012; 149:1192–1205.
20. Vladar EK, Antic D, Axelrod JD. Planar cell polarity signaling: the developing cell's compass. *Cold Spring Harb Perspect Biol* 2009;1: a002964.
21. Vladar EK, Bayly RD, Sangoram AM, Scott MP, Axelrod JD. Microtubules enable the planar cell polarity of airway cilia. *Curr Biol* 2012;22:2203–2212.
22. Benjamini Y, Hochberg Y. Controlling the false discovery rate - a practical and powerful approach to multiple testing. *J R Stat Soc B* 1995;57:289–300.
23. Benjamini Y, Yekutieli D. False discovery rate-adjusted multiple confidence intervals for selected parameters. *J Am Stat Assoc* 2005; 100:71–81.
24. Vladar EK, Brody SL. Analysis of ciliogenesis in primary culture mouse tracheal epithelial cells. *Methods Enzymol* 2013;525:285–309.
25. Lilien J, Balsamo J. The regulation of cadherin-mediated adhesion by tyrosine phosphorylation/dephosphorylation of β-catenin. *Curr Opin Cell Biol* 2005;17:459–465.
26. Rhee J, Buchan T, Zukerberg L, Lilien J, Balsamo J. Cables links Robo-bound Abl kinase to N-cadherin-bound β-catenin to mediate Slit-induced modulation of adhesion and transcription. *Nat Cell Biol* 2007;9:883–892.
27. Jho EH, Zhang T, Domon C, Joo CK, Freund JN, Costantini F. Wnt/β-catenin/Tcf signaling induces the transcription of Axin2, a negative regulator of the signaling pathway. *Mol Cell Biol* 2002;22:1172–1183.
28. Bernard P, Fleming A, Lacombe A, Harley VR, Vilain E. Wnt4 inhibits β-catenin/TCF signalling by redirecting β-catenin to the cell membrane. *Biol Cell* 2008;100:167–177.
29. Coombs GS, Covey TM, Virshup DM. Wnt signaling in development, disease and translational medicine. *Curr Drug Targets* 2008;9:513–531.
30. Polakis P. Wnt signaling in cancer. *Cold Spring Harb Perspect Biol* 2012;4:a008052.
31. Fulcher ML, Randell SH. Human nasal and tracheo-bronchial respiratory epithelial cell culture. *Methods Mol Biol* 2013;945: 109–121.
32. Kalluri R. EMT: when epithelial cells decide to become mesenchymal-like cells. *J Clin Invest* 2009;119:1417–1419.
33. Kalluri R, Weinberg RA. The basics of epithelial-mesenchymal transition. *J Clin Invest* 2009;119:1420–1428.
34. Hupin C, Gohy S, Bouzin C, Lecocq M, Polette M, Pilette C. Features of mesenchymal transition in the airway epithelium from chronic rhinosinusitis. *Allergy* 2014;69:1540–1549.
35. Vladar EK, Nayak JV, Milla CE, Axelrod JD. Airway epithelial homeostasis and planar cell polarity signaling depend on multiciliated cell differentiation. *JCI Insight* 2016;1:e88027.
36. Shahana S, Jaunmuktane Z, Asplund MS, Roomans GM. Ultrastructural investigation of epithelial damage in asthmatic and non-asthmatic nasal polyps. *Respir Med* 2006;100:2018–2028.
37. Jang YJ, Kim HG, Koo TW, Chung PS. Localization of ZO-1 and E-cadherin in the nasal polyp epithelium. *Eur Arch Otorhinolaryngol* 2002;259:465–469.
38. Wladislavosky-Waserman P, Kern EB, Holley KE, Eisenbrey AB, Gleich GJ. Epithelial damage in nasal polyps. *Clin Allergy* 1984;14:241–247.
39. Soyka MB, Wawrzyniak P, Eiwegger T, Holzmann D, Treis A, Wanke K, Kast JI, Akdis CA. Defective epithelial barrier in chronic rhinosinusitis: the regulation of tight junctions by IFN-γ and IL-4. *J Allergy Clin Immunol* 2012;130:1087–1096.e10.
40. Okubo T, Hogan BL. Hyperactive Wnt signaling changes the developmental potential of embryonic lung endoderm. *J Biol* 2004;3:11.
41. Mucenski ML, Nation JM, Thitoff AR, Besnard V, Xu Y, Wert SE, Harada N, Taketo MM, Stahlman MT, Whitsett JA. β-catenin regulates differentiation of respiratory epithelial cells *in vivo*. *Am J Physiol Lung Cell Mol Physiol* 2005;289:L971–L979.

42. Mucenski ML, Wert SE, Nation JM, Loudy DE, Huelsken J, Birchmeier W, Morrisey EE, Whitsett JA. β-catenin is required for specification of proximal/distal cell fate during lung morphogenesis. *J Biol Chem* 2003;278:40231–40238.
43. Douglas IS, Diaz del Valle F, Winn RA, Voelkel NF. β-catenin in the fibroproliferative response to acute lung injury. *Am J Respir Cell Mol Biol* 2006;34:274–285.
44. Park KS, Wells JM, Zorn AM, Wert SE, Laubach VE, Fernandez LG, Whitsett JA. Transdifferentiation of ciliated cells during repair of the respiratory epithelium. *Am J Respir Cell Mol Biol* 2006;34:151–157.
45. Lam AP, Flozak AS, Russell S, Wei J, Jain M, Mutlu GM, Budinger GR, Feghali-Bostwick CA, Varga J, Gottardi CJ. Nuclear β-catenin is increased in systemic sclerosis pulmonary fibrosis and promotes lung fibroblast migration and proliferation. *Am J Respir Cell Mol Biol* 2011;45:915–922.
46. Baniyash M. TCR ξ-chain downregulation: curtailing an excessive inflammatory immune response. *Nat Rev Immunol* 2004;4:675–687.
47. Meng J, Zhou P, Liu Y, Liu F, Yi X, Liu S, Holtappels G, Bachert C, Zhang N. The development of nasal polyp disease involves early nasal mucosal inflammation and remodelling. *PLoS One* 2013;8: e82373.
48. Xiao C, Puddicombe SM, Field S, Haywood J, Broughton-Head V, Puxeddu I, Haitchi HM, Vernon-Wilson E, Sammut D, Bedke N, *et al*. Defective epithelial barrier function in asthma. *J Allergy Clin Immunol* 2011;128:549–556.e1–12.
49. Tilley AE, Walters MS, Shaykhiev R, Crystal RG. Cilia dysfunction in lung disease. *Annu Rev Physiol* 2015; 77:379–406.
50. Flozak AS, Lam AP, Russell S, Jain M, Peled ON, Sheppard KA, Beri R, Mutlu GM, Budinger GR, Gottardi CJ. β-catenin/T-cell factor signaling is activated during lung injury and promotes the survival and migration of alveolar epithelial cells. *J Biol Chem* 2010;285: 3157–3167.